Neurobiology of Disease 124 (2019) 81–92

Contents lists available at ScienceDirect

Neurobiology of Disease

journal homepage: www.elsevier.com/locate/ynbdi

Microsomal prostaglandin E synthase-1 is a critical factor in dopaminergic neurodegeneration in Parkinson's disease

Yuri Ikeda-Matsuo[a,b,*], Hajime Miyata[c], Tomoko Mizoguchi[b], Eisaku Ohama[d], Yasuhito Naito[b], Satoshi Uematsu[e,f], Shizuo Akira[g], Yasuharu Sasaki[b], Mitsuo Tanabe[b]

[a] Laboratory of Pharmacology, Department of Clinical Pharmacy, Faculty of Pharmaceutical Sciences, Hokuriku University, Japan
[b] Laboratory of Pharmacology, School of Pharmaceutical Sciences, Kitasato University, Japan
[c] Department of Neuropathology, Research Institute for Brain and Blood Vessels – AKITA, Japan
[d] Kurashiki Heisei Hospital, Japan
[e] Department of Mucosal Immunology, School of Medicine, Chiba University, Japan
[f] Division of Innate Immune Regulation, International Research and Development Center for Mucosal Vaccines, The Institute of Medical Science, The University of Tokyo, Japan
[g] Laboratory of Host Defense, WPI Immunology Frontier Research Center, Osaka University, Japan

ARTICLE INFO

Keywords:
Parkinson's disease
Neurodegeneration
Prostaglandin E_2
Microsomal prostaglandin E synthase
Neuroinflammation
Dopamine
Neurotoxicity
Lewy bodies
6-hydroxydopamine

ABSTRACT

Parkinson's disease (PD) is a neurodegenerative disorder of uncertain pathogenesis characterized by the loss of nigrostriatal dopaminergic neurons. Although increased production of prostaglandin E_2 (PGE_2) has been implicated in tissue damage in several pathological settings, the role of microsomal prostaglandin E synthase-1 (mPGES-1), an inducible terminal enzyme for PGE_2 synthesis, in dopaminergic neurodegeneration remains unclear. Here we show that mPGES-1 is up-regulated in the dopaminergic neurons of the substantia nigra of postmortem brain tissue from PD patients and in neurotoxin 6-hydroxydopamine (6-OHDA)-induced PD mice. The expression of mPGES-1 was also up-regulated in cultured dopaminergic neurons stimulated with 6-OHDA. The genetic deletion of mPGES-1 not only abolished 6-OHDA-induced PGE_2 production but also inhibited 6-OHDA-induced dopaminergic neurodegeneration both in vitro and in vivo. Nigrostriatal projections, striatal dopamine content, and neurological functions were significantly impaired by 6-OHDA administration in wild-type (WT) mice, but not in mPGES-1 knockout (KO) mice. Furthermore, in cultured primary mesencephalic neurons, addition of PGE_2 to compensate for the deficiency of 6-OHDA-induced PGE_2 production in mPGES-1 KO neurons recovered 6-OHDA toxicity to almost the same extent as that seen in WT neurons. These results suggest that induction of mPGES-1 enhances 6-OHDA-induced dopaminergic neuronal death through excessive PGE_2 production. Thus, mPGES-1 may be a valuable therapeutic target for treatment of PD.

1. Introduction

Parkinson's disease (PD) is one of the most common age-related neurodegenerative disorders and is characterized by the loss of nigrostriatal dopaminergic neurons and cardinal motor symptoms (Magrinelli et al., 2016). Although many effective treatments are currently available that mostly address motor symptoms, no known curative therapy exists to date, and thus, effective treatments that will stop or slow disease progression are urgently needed. Recently, extensive investigations including epidemiologic, animal, human, and therapeutic studies have revealed that neuroinflammation plays a key role in the initiation and progression of PD (Tufekci et al., 2012; Deleidi and Gasser, 2013).

Prostaglandin E_2 (PGE_2), one of the most likely candidates for the propagation of inflammation, is known to be accumulated in the substantia nigra (SN) of postmortem brains from parkinsonian patients and in toxin-induced animal models of PD (Mattammal et al., 1995; Yildirim et al., 2014; Teismann et al., 2003). PGE_2 is sequentially synthesized

Abbreviations: PD, Parkinson's disease; PGE_2, prostaglandin E_2; mPGES-1, microsomal prostaglandin E synthase; 6-OHDA, 6-hydroxydopamine; WT, wild-type; KO, knock out; COX, cyclooxygenase; MPTP, 1 methyl-4-phenyl-1,2,3,6 terahydropyridine; PGI_2, prostaglandin I_2; PGD_2, prostaglandin D_2; TXA_2, thromboxane A_2; cPGES, cytosolic PGES; DA, dopamine; SNpc, substantia nigra pars compacta

* Corresponding author at: Laboratory of Pharmacology, Department of Clinical Pharmacy, Faculty of Pharmaceutical Sciences, Hokuriku University, Ho-3 Kanagawa-machi, Kanazawa 920-1181, Japan.
E-mail address: y-matsuo@hokuriku-u.ac.jp (Y. Ikeda-Matsuo).

https://doi.org/10.1016/j.nbd.2018.11.004
Received 30 May 2018; Received in revised form 1 November 2018; Accepted 9 November 2018
Available online 10 November 2018
0969-9961/

from arachidonic acid by two enzymatic steps via cyclooxygenase (COX) and PGE_2 synthase (PGES). Among the COX isoforms, COX-2 is the inducible form; however, it has been immunohistochemically detected in neurons in the normal brain (Kaufmann et al., 1997). COX-2 has been demonstrated to be up-regulated in dopaminergic neurons in PD specimens and in neurotoxin, 1-methyl-4-phenyl-1,2,4,6-tetrahydropyridine (MPTP) and 6-hydroxydopamine (6-OHDA)-induced animal models of PD (Teismann et al., 2003; Lima et al., 2006). The genetic disruption and chemical inhibition of COX-2 have been shown to ameliorate dopaminergic neuronal death in toxin-induced animal models of PD, suggesting that PGE_2 accumulated through COX-2 induction mediates the toxic effects in the brain (Teismann et al., 2003; Reksidler et al., 2007; Sánchez-Pernaute et al., 2004). As COX-2 produces not only PGE_2, but also PGI_2, PGD_2, $PGF_{2\alpha}$, and thromboxane (TX) A_2 by coordination with PGIS, PGDS, PGFS, and TXAS, respectively, inhibition of prostanoids other than PGE_2 may contribute to the neuroprotective effects of genetic deletion or pharmacological inhibition of COX-2. COX-2 also enzymatically oxidizes dopamine (DA) to DA quinone by its peroxidase activities, which is suggested to contribute to dopaminergic neurodegeneration through oxidative stress and mitochondrial dysfunction (Mattammal et al., 1995; Asanuma and Miyazaki, 2006). Contrary to the suggested neurotoxic effects of PGE_2, stimulation of one of the PGE_2 receptors, EP2, has been reported to protect dopaminergic neurons against 6-OHDA toxicity in a primary neuronal culture (Carrasco et al., 2008). Therefore, the study of PGES, a terminal enzyme for PGE_2 synthesis, should provide sufficient information to help resolve this uncertainty regarding the role of endogenous PGE_2.

Three major isoforms of PGES have been isolated: cytosolic PGES (cPGES), microsomal PGES (mPGES)-1, and mPGES-2. While cPGES and mPGES-2 are constitutively expressed in various cells and tissues, mPGES-1 is induced by proinflammatory stimuli and in various models of inflammation, and is functionally coupled to COX-2 (Jakobsson et al., 1999; Murakami et al., 2000). The profile of mPGES-1 knockout (KO) mice, such as reduction in PGE_2 production, inhibition of tissue inflammation and amelioration of insults, strongly supports the notion that mPGES-1 plays an important role in inflammatory PGE_2 production and in the inflammation seen in animal models of pain, arthritis, and pyrexia (Uematsu et al., 2002; Engblom et al., 2003; Kamei et al., 2004).

Recently, we demonstrated that the induction of mPGES-1 contributes to neuronal death and neurological deficits following brain ischemia (Ikeda-Matsuo et al., 2006). Thus, we hypothesized that mPGES-1 could be a common accelerating factor with respect to neuronal death in inflammatory brain diseases, including PD. Here, we show that mPGES-1 is induced in dopaminergic neurons in the SN of postmortem brains from PD patients and in 6-OHDA-induced PD mice. We also show that co-induction of mPGES-1 and COX-2 contributes not only to excessive PGE_2 production in the SN, but also to dopaminergic neurodegeneration, loss of nigrostriatal projections, and behavioral neurological dysfunction in 6-OHDA-induced PD mice.

2. Materials and methods

2.1. Animals

Male (22–27 g) mPGES-1 knockout (KO) mice, and male and female (20–24 g) wild-type (WT) mice (C57BL/6 J × 129/SvJ background) back-crossed to C57BL/6 J mice for > eight generations to avoid artifactual differences caused by genetic background were used (Uematsu et al., 2002). For the in vitro study, pregnant female mPGES-1 KO and WT mice at E15 were used. All experiments were carried out in accordance with the guidelines given by the Japanese Pharmacological Society, and protocols were approved by the Institutional Animal Care and Use Committee at Kitasato University and Hokuriku University.

2.2. 6-OHDA lesion

Dopaminergic neurons were destroyed unilaterally by local administration of the neurotoxin 6-OHDA into the striatum. Mice were anesthetized by halothane and 2 μL of a 2 μg/μL 6-OHDA (Sigma) solution (dissolved in physiological saline with 0.1% ascorbic acid) was injected into the left striatum (−0.6 mm posterior, 1.5 mm lateral, and 3.0 mm ventral from bregma). Injections were delivered using a Hamilton needle over a period of 4 min, and the needle was left in place for a further 4 min. The right striatum received 2 μL of vehicle (saline in 0.1% ascorbic acid) at the same coordinates and was used as a sham control. Additionally, sham-operated mice were infused with 2 μL of vehicle into both the right and left striata and served as controls in the rotarod test. Animals were euthanized for analysis at 1, 3, 7, 14, and 21 days after surgery.

2.3. Mesencephalic neuronal culture

Cultures of primary neurons were established as previously described (Ikeda et al., 1997) with minor modifications. Briefly, ventral mesencephalon of embryonic day 15 WT or mPGES-1 KO mice was dissected free of meninges in ice-cold L-15 medium and minced with two scalpels. It was then incubated with a mixture of 0.25% trypsin (Difco, 1:250) and 0.01% deoxyribonuclease I (Sigma-Aldrich) at 37 °C for 15 min. The incubation was terminated by addition of horse serum (Invitrogen). The tissue fragments were centrifuged at 1200 rpm for 5 min. The pellet was resuspended in modified Eagle's medium containing 10% FBS and single cells were dissociated by gentle pipetting and passing through two sheets of nylon net (25-μm mesh). The dissociated cells were plated at an initial density of 5×10^5 cells/cm^2 onto 96-well plates or 2.5×10^5 cells/cm^2 onto a 35-mm dish (Corning) pretreated for one day with 0.1 mg/mL poly-L-lysine hydrochloride (Sigma-Aldrich) dissolved in 0.15 M borate buffer. They were cultured for seven days at 37 °C in a humidified 5% CO_2–95% air atmosphere. Half of the culture medium was changed every 3 days.

2.4. Western blotting

The SN dissected from the lesioned or sham-operated brain or cultured mesencephalic neurons were lysed by homogenization in 10 mM HEPES-buffered solution (pH 7.4) containing 5 mM EDTA, 1 mM dithiothreitol, 1× protease inhibitor mixture (Nacalai) and 50% (v/v) glycerol, followed by sonication three times for 10 s, and centrifugation at 15,000 ×*g* for 10 min at 4 °C. The protein concentration in the supernatants was measured using the Bradford method. A total of 4 μg of protein from each sample was denatured by boiling for 5 min in sample buffer (62.5 mM Tris-HCl, pH 6.7, 1% (*w/v*) SDS, 10% (v/v) glycerol, 2% (v/v) 2-mercaptoethanol, 0.025% (w/v) bromophenol blue), separated by electrophoresis using 15% SDS–polyacrylamide gels, and transferred electrophoretically onto immobilon-P polyvinylidene difluoride membranes (Millipore). The membranes were blocked overnight in 5% skimmed milk/Tris-buffered saline–Tween 20 (TBS–T; 10 mM Tris-HCl, pH 7.4, containing 150 mM NaCl, 0.1% Tween 20). The membranes were incubated with the appropriate primary antibodies against mPGES-1 (Cayman; 1:200 dilution), mPGES-2 (Cayman; 1:250), cPGES (Cayman; 1:250), COX-1 (Cayman; 1:250), COX-2 (Santa Cruz; 1:250), and β-actin (Sigma-Aldrich, 1:5000) in Solution 1 of the Can Get Signal kit (Toyobo) for 1.5 h. After washing the membranes with TBS–T, horseradish peroxidase-conjugated secondary antibodies (Jackson ImmunoResearch) were added at a 1:10,000 dilution in Solution 2 of the Can Get Signal kit and were incubated for 1 h. After washes with TBS–T, the protein bands were visualized using Chemi-Lumi One western blot detection reagents (Nacalai) and detected by a Light-Capture system (Atto).

2.5. Real-time PCR

RNA extraction from the SN was performed as described (Ikeda et al., 2000). Briefly, total RNA was extracted with Sepasol (Nacalai) and then treated with RNase-free DNase I for 15 min at room temperature. Two μg of total RNA was reverse-transcribed using High-Capacity cDNA Reverse Transcription Kits (Applied Biosystems). Expression of mPGES-1 mRNA was quantified by real-time PCR using the 7900HT Fast Real-Time PCR System (Applied Biosystems) with SYBR Premix Ex Taq (Takara). After amplification (one cycle at 95 °C for 1 min and 40 cycles at 95 °C for 15 s, 60 °C for 1 min), a melting curve was constructed to determine the melting temperature of each PCR product. The mRNA levels of each gene of interest and of β-actin, chosen as a housekeeping gene, were determined in parallel for each sample. Results are expressed as the normalized ratio of the mRNA level of the mPGES-1 gene over the β-actin gene. The inductions of mPGES-1 were visualized by semi-quantitative PCR methods (one cycle at 94 °C for 3 min and 34 cycles for mPGES-1 or 25 cycles for β-actin at 94 °C for 30 s, 60 °C for 30 s, 72 °C for 45 s, one cycle at 72 °C for 5 min). Inductions and sizes were checked on a 2% agarose gel stained with ethidium bromide. The gene-specific primer pairs used for real-time PCR were as follows: mPGES-1, sense 5′-ATCAAGATGTACGCGGT GGC-3′, antisense 5′-GAGGAAATGTATCCAGGCGA-3′; β-actin, sense 5′-TCCTCCTGAGCGCAAGTACTCT-3′, antisense 5′-GCTCAGTAACAGT CCGCCTAGAA-3′.

2.6. Staining of mouse brain slices

Animals were anesthetized with sodium pentobarbital (50 mg/kg, i.p.) and then perfused transcardially with saline, followed by 4% paraformaldehyde in PBS. The brains were removed, post-fixed overnight in a solution containing 4% paraformaldehyde and 4% sucrose in PBS, and then cryoprotected for 1 day each in solutions containing 10% and 20% sucrose in PBS. The brains were then embedded in optimal cutting temperature compound (Sakura Finetek) and frozen in dry-ice powder before coronal sections (20 μm) were cut using a cryostat. The sliced tissues were permeabilized with 0.3% Triton X-100 for 10 min and then treated with 3% BSA in PBS for 15 min to block nonspecific binding. The preparations were incubated with the appropriate primary antibodies against mPGES-1 (Cayman; 1:200 dilution), COX-2 (Santa Cruz; 1:250), tyrosine hydroxylase (TH, Sigma-Aldrich; 1:300), CD11b (Serotec; 1:50), neuron-specific nuclear protein (Neu−N, Chemicon; 1:2000), and glial fibrillary acidic protein (GFAP, Sigma-Aldrich; 1:1000) in PBS containing 3% albumin at 4 °C overnight, and were washed in PBS. The preparations were incubated with Cy3- or FITC-conjugated secondary antibodies (Jackson ImmunoResearch; 1:100). The slices were mounted with Vectashield Mounting Medium (Vector Laboratories) and examined using a confocal laser scanning system (LSM 510) on an Axiovert 200 M inverted microscope (Carl Zeiss) or a Biozero fluorescence microscope (Keyence). TH-, Neu-N-, CD11b-, GFAP- and mPGES-1-positive cells in the SN of coronal brain slices (-3.0 ± 0.05 mm posterior from bregma) were counted using ImageJ software.

2.7. Prostanoid and 8-isoprostane assay

The SN was dissected from the brain, quickly frozen in liquid nitrogen, and weighed to determine the wet weight. Prostanoids were extracted by homogenization of the tissue in a 70% methanol solution containing 10 μM indomethacin and centrifugation at 15,000 $\times g$ for 20 min at 4 °C. The supernatant was evaporated and dissolved with the assay buffer. For the in vitro assay, the culture medium was directly diluted with the assay buffer. The concentrations of PGE_2, 6-keto $PGF_{1\alpha}$, PGD_2, TXB_2, and 8-isoprostane in extracts or culture medium were determined according to the protocol of the enzyme immunoassay kit (Cayman). For PGD_2 measurement, PGD_2 was converted to a stable methoxime derivative before conducting immunoassay.

2.8. Human brain postmortem study

Formalin-fixed and paraffin-embedded archival blocks of the midbrain were chosen from seven cases of autopsy-confirmed PD (male:female = 1:7; age at death 66–90 years old) and four control cases without neurological disease (male:female = 4:0; age at death 40–80 years old). Seven-μm thick sections were cut and mounted on silane-coated glass slides. Routine sections were stained with hematoxylin and eosin. Double-label immunohistochemistry was performed using a monoclonal antibody against α-synuclein (clone LB509, dilution 1:35, a kind gift from Dr. T. Iwatsubo (Baba et al., 1998)) as the first immunostaining for Lewy bodies, and rabbit polyclonal antibodies against mPGES-1 (Cayman; 1:100 dilution) as the second immunostaining, using a labeled polymer method (goat antimouse or antirabbit immunoglobulins conjugated to a peroxidase labeled-dextran polymer, EnVision+ System-HRP, Dako) with a combination of 3,3′-diaminobenzidine tetrahydrochloride (DAB, Dako) and an acetonitrile compound (SG, Vector Laboratories) as chromogens. For each immunostaining, deparaffinized sections were subjected to antigen retrieval by boiling in a 0.015 M sodium citrate buffer (pH 6.0) for 12 min using a household microwave oven. Sections were incubated with primary antibodies for 20 min under continuous microwave irradiation (200 watts, Azumaya Microwave Processor MI-77, Azumaya Inc.) at approximately 25–37 °C. Sections were finally counterstained with Nuclear Fast Red (Vector Laboratories). Immunostaining with omission of primary antibodies was used as a negative control. Cell counting was performed in the bilateral SN in the horizontal section of the midbrain at the level of the superior colliculi. The positive ratio of mPGES-1 was evaluated on the mPGES-1 immunostained sections, and defined as the percentage of mPGES-1-immunoreactive neurons among the total number of neurons in the bilateral SN.

2.9. Immunocytochemistry

Cultured cells were fixed with 4% PFA in PBS for 30 min, permeabilized with 0.01% saponin in PBS for 3 min, and then treated with 1% BSA in PBS for 15 min to block nonspecific binding. The cells were incubated with primary antibodies against mPGES-1 (1:200 dilution), TH (1:300), and MAP-2 (Sigma-Aldrich; 1:200) in PBS containing 1% albumin at 4 °C overnight. After washing with PBS, the cells were incubated with Cy3- or FITC-conjugated secondary antibodies (1:100) and then mounted with Vectashield Mounting Medium. The stained cells were examined as for the stained brain slices described above. TH-positive cells in the well (33 mm^2) were counted using ImageJ software.

2.10. MTT assay

The toxicity of 6-OHDA in mesencephalic neurons was determined by the MTT assay. After treatment with 5 or 30 μM 6-OHDA for 6–72 h, 10 μL of a 2.5 mg/mL MTT stock solution was added to each well containing 100 μL of medium; the reaction mixture was then incubated for 2 h. The reaction was stopped by adding 100 μL of a solution containing 50% dimethylformamide and 20% SDS (pH 4.7). After overnight incubation at 37 °C, the absorbance was measured using a microplate reader at a test wavelength of 570 nm and a reference wavelength of 655 nm (iMark, Bio-Rad).

2.11. Retrograde labeling with Fluoro-Gold

Nine days after unilateral 6-OHDA injection, rats received bilateral FG (Hydroxystilbamidine, Sigma) injections (0.1 μg/2 μL) into the striatum as for 6-OHDA injection. Retrograde labeling of SN neurons was examined using a confocal laser scanning system (LSM 510, Carl Zeiss) 5 days later.

2.12. Measurement of DA content

Mouse brains were immediately dissected following decapitation to isolate the striatum, and the weight of the tissue was recorded. After adding isoproterenol, an internal control, the striatum was homogenized in 200 μL of 0.02 M perchloric acid containing 100 μM EDTA, followed by sonication three times for 10 s, and centrifugation (15,000 ×*g* for 15 min at 4 °C) to remove proteins. After filtration of the supernatant (0.45 μm, pH 3 with CH_3COONa), 0.02 M CH_3COOH was added and the amounts of DA, 5-HT and their metabolites DOPAC, HVA, and 5-HIAA in the supernatant were detected using the HPLC-ECD method (HTEC-500, SC-5ODS column, Eicom).

2.13. Rotarod test

Rotarod testing with a rod diameter of 3 cm (Muromachi) was performed 14 days after surgery, at 16 rpm for 1 min followed by 20 rpm for 4 min. All mice were pre-trained 1 day before lesioning. The training consisted of three runs, with an inter-trial interval of 3 h, at 16 rpm for 1 min followed by 20 rpm for 1 min. On the next day, mice were trained again just before surgery at 16 rpm for 1 min followed by 20 rpm for 4 min, and the mice that fell in 5 min were excluded from the experiment.

2.14. Statistical analysis

Results are expressed as the mean ± standard error of the mean. Statistical significance was evaluated using one-way analysis of variance followed by Tukey's method. $P < .05$ was considered statistically significant.

3. Results

3.1. mPGES-1 is induced in dopaminergic neurons of the SN in 6-OHDA-lesioned mice

To determine whether the expression of PGES as well as the COX isoforms is affected during nigrostriatal neurodegeneration, we assessed PGES and COX content in the SN of sham-operated and 6-OHDA-lesioned mice at different time points. mPGES-1 protein levels gradually increased from three days, and by 14–21 days, expression had reached a maximal level that was approximately four-fold higher than that seen in sham-operated animals (Fig. 1A). mPGES-2, cPGES, COX-1, and COX-2 proteins were constitutively expressed and there were no significant differences between the SN of sham and lesioned mice. The mRNA of mPGES-1 in the SN was also up-regulated at 14 days after 6-OHDA injection, compared to sham-operated mice (Fig. 1B). A significant accumulation of PGE_2 was detected at three days after 6-OHDA injection and had returned to basal levels at seven days (Fig. 1C). In female mice, the expression of mPGES-1 mRNA was significantly increased at 14 days after 6-OHDA injection to a similar level as that in male mice; Male-SHAM, 1.00 ± 0.12; Male-6-OHDA, 2.67 ± 1.28 and Female-SHAM, 0.99 ± 0.13; Female-6-OHDA, 2.13 ± 0.20 ($p < .01$ vs Female-SHAM, n = 5). The production of PGE_2 in female mice brain at 3 days after 6-OHDA injection was also up-regulated, but it was less than that in male mice brain and not significant; PGE_2 in ng/g tissue; Male-SHAM, 4.07 ± 0.44; Male-6-OHDA, 10.32 ± 1.92 ($p < .05$ vs Male-SHAM) and Female-SHAM, 3.04 ± 0.13; Female-6-OHDA, 5.82 ± 1.34. Immunostaining for mPGES-1 in mouse brain slices revealed that mPGES-1 was induced in the SN pars compacta (SNpc) of 6-OHDA-lesioned WT mice, but not in mPGES-1 KO mice (Fig. 2A). Immunostaining for mPGES-1 and COX-2 revealed co-induction and co-localization of these proteins in the SNpc of 6-OHDA-lesioned mice (Fig. 2B). Most of the mPGES-1-positive cells were positive for neuron-specific nuclear protein Neu-N and TH, specific markers for neurons and dopaminergic neurons, respectively (Fig. 2C, Table 1). High magnification clearly showed that mPGES-1 and either COX-2, Neu−-N, or TH were expressed in the same cells (inset of Fig. 2B,C). None of the mPGES-1-positive cells were positive for CD11b or GFAP, specific markers for microglia and astrocytes, respectively. These results indicate that the mPGES-1 protein is induced in at least a portion of the dopaminergic neurons during nigrostriatal neurodegeneration.

3.2. mPGES-1 is up-regulated in dopaminergic neurons in the SNpc of postmortem brains from PD patients

To determine whether the changes in mPGES-1 seen in 6-OHDA-lesioned mice were present in PD patients, we assessed mPGES-1 protein content in postmortem SNpc samples (Table 2). In all cases with autopsy-confirmed PD, the SN showed marked neuronal loss and fibrillary gliosis (Fig. 3A), with scattered free melanin and melanin-laden macrophages (data not shown) as well as Lewy bodies in the remaining

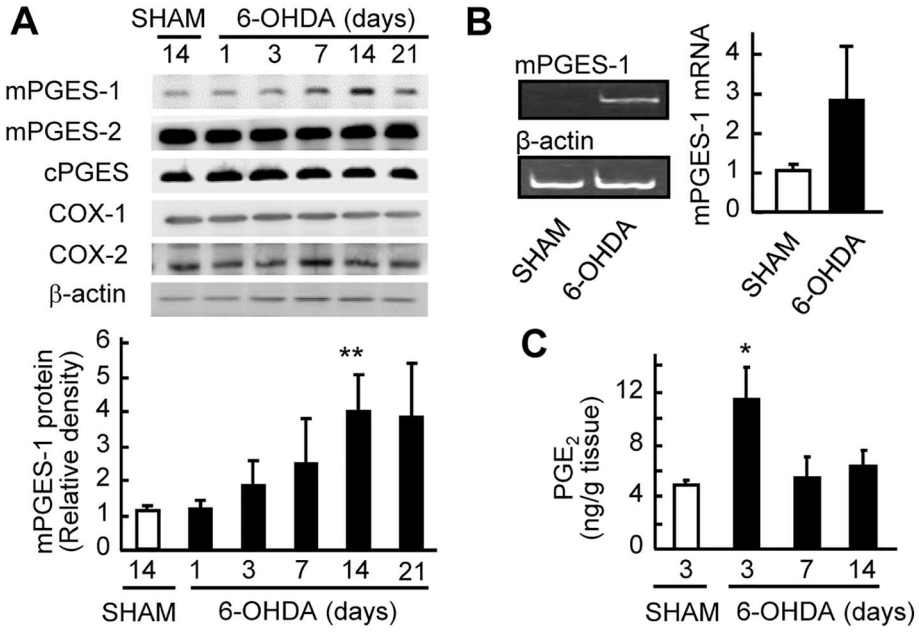

Fig. 1. mPGES-1 induction and PGE_2 production in the SN in 6-OHDA-lesioned mice. A, Western blot analysis of the expression of enzymes related to PGE_2 synthesis in the SN at the indicated time after 6-OHDA injection and 14 days after a sham operation (SHAM). Bar graph: Quantitated data from immunoblotting with the mPGES-1 antibody were normalized to β-actin; n = 4–6, $^{**}p < .01$ vs. SHAM. B, Real-time PCR analysis of the expression of mPGES-1 mRNA in the SN at 14 days after 6-OHDA injection. Bar graph: Quantitated data for mPGES-1 mRNA expression were normalized to those for β-actin; n = 4. Images: Representative band images of mPGES-1 mRNA from SN at 14 days after 6-OHDA injection were taken from agarose gel visualization by semi-quantitative PCR; n = 3. C, The amount of PGE_2 in the SN after 6-OHDA injection and three days after a sham operation (SHAM); n = 4, $^{*}p < .05$ vs. SHAM.

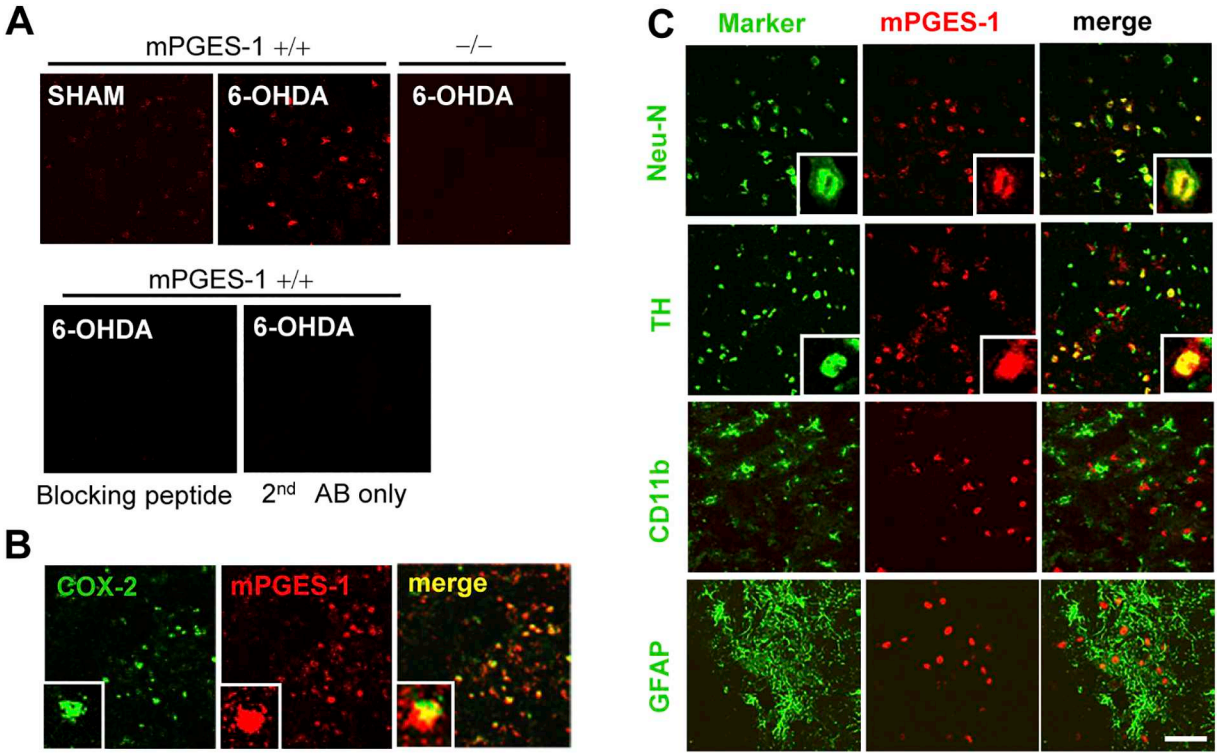

Fig. 2. Co-induction of mPGES-1 with COX-2 in dopaminergic neurons in the SN in 6-OHDA-lesioned mice. A, Immunostaining of mPGES-1 in the SN at 14 days after 6-OHDA and vehicle (SHAM) injection in WT (+/+) and mPGES-1 KO (−/−) mice. Specificity of mPGES-1 antibody was confirmed by preabsorbed mPGES-1 antibody using blocking peptide or without the mPGES-1 antibody (lower photos). B, Double-immunostaining of mPGES-1 (red) and COX-2 (green) in the SN at 14 days after 6-OHDA injection in WT mice. C, Double-immunostaining of mPGES-1 (red) and cell-type-specific marker proteins (green) in the SN at 14 days after 6-OHDA injection. Neurons, dopaminergic neurons, microglia, and astrocytes were recognized by antibodies for Neu-N, TH, CD11b, and GFAP, respectively. Representative immunohistochemical pictures are shown (n = 4). Scale bar, 50 μm; insets, 12.5 μm. (For interpretation of the references to colour in this figure legend, the reader is referred to the web version of this article.)

Table 1
Changes in the number of Neu−N−, TH-, CD11b- and GFAP-mPGES-1-positive cells in the substantia nigra of 6-OHDA-lesioned mice.

		SHAM	6-OHDA
Neu-N	Neu-N(+)	46.0 ± 1.4	5.3 ± 2.3**
	mPGES-1(+)	6.0 ± 5.4	0.3 ± 0.3
	Neu-N(+)/mPGES-1(+)	2.0 ± 0.8	22.8 ± 1.9**
TH	TH(+)	49.3 ± 5.7	9.3 ± 1.7**
	mPGES-1(+)	1.0 ± 0.7	3.8 ± 1.4
	TH(+)/mPGES-1(+)	4.3 ± 2.7	23.3 ± 2.8**
CD11b	CD11b(+)	28.5 ± 3.9	39.8 ± 6.9
	mPGES-1(+)	1.3 ± 0.6	25.0 ± 3.2**
	CD11b(+)/mPGES-1(+)	0.0 ± 0.0	0.8 ± 0.5
GFAP	GFAP(+)	57.3 ± 7.6	79.8 ± 9.3
	mPGES-1(+)	0.3 ± 0.3	19.3 ± 2.6**
	GFAP(+)/mPGES-1(+)	1.0 ± 0.7	1.0 ± 0.6

The number of positive cells were counted in microscopic fields (40,000 μm^2, Fig. 2); n = 4, $^{**}p < .01$ vs. SHAM.

neurons (Fig. 3B). Most remaining neurons showed diffuse cytoplasmic immunoreactivity for mPGES-1 (Fig. 3C,D), regardless of the presence or absence of α-synuclein-positive Lewy bodies. On rare occasions, some neurons showed multiple cytoplasmic Lewy bodies without cytoplasmic mPGES-1 immunoreactivity (Fig. 3E); however, relatively weak but diffuse cytoplasmic immunoreactivity for α-synuclein was also noted in such neurons. The expression of mPGES-1 was also observed in neurites. In addition to the α-synuclein-immunoreactive Lewy-related neurites, small Lewy bodies were also observed within mPGES-1-positive neurites (Fig. 3F,G). In contrast, mPGES-1-positive neurons in control cases constituted a minor component among the total number of neurons in the SN (Fig. 3H). The similarity of the mPGES-1 alterations between the 6-OHDA-lesioned mice and the PD postmortem specimens strengthens the value of using this experimental model to study the role of mPGES-1 in the PD neurodegenerative process.

3.3. Up-regulation of mPGES-1 contributes to PGE_2 production and dopaminergic neuronal death induced by 6-OHDA in mesencephalic neuronal cultures

To investigate the role of dopaminergic neuronal mPGES-1 in 6-OHDA-induced PGE_2 production and neuronal death, we cultured mesencephalic dopaminergic neurons from WT and mPGES-1 KO embryos. mPGES-1 protein levels were gradually increased after 30 μM 6-OHDA treatment, and by 48 h, expression had reached a maximal level that was about 2.5-fold higher than in the control (Fig. 4A). On the other hand, protein expressions of mPGES-2, cPGES, COX-1, and COX-2 were not increased by 6-OHDA until 48 h (data not shown). The expression of mPGES-1 mRNA was also increased at 24 h after 6-OHDA treatment, being > 10-fold higher than in the control (Fig. 4B). Immunostaining for mPGES-1 also showed its induction by 6-OHDA in WT neurons, although no mPGES-1-positive staining was observed in neurons derived from mPGES-1 KO mice (Fig. 4C). The immunostaining of mPGES-1 observed in 6-OHDA-treated WT neurons was abolished by staining with the mPGES-1-antibody preabsorbed with the antigen mPGES-1 peptide or by staining without the mPGES-1-antibody (data not shown). The mPGES-1-positive cells were also positive for MAP-2 and partially positive for TH (Fig. 4D), indicating that mPGES-1 is induced in not only dopaminergic neurons, but also non-dopaminergic and/or immature neurons which have undetectable levels of TH. In WT neurons, PGE_2 production was gradually increased after 6-OHDA treatment, and

Table 2
Postmortem human midbrain specimens from autopsy-confirmed PD patients and control cases without neurological disease.

	No.	Age/Sex	Final diagnosis	Clinical duration (y)	Brain weight (g)	mPGES-1 (+) cells	Total neuronal cells	Positive ratio (%)
PD	1	66F	PD	27	1420	102	148	68.9
	2	71F	PD	10	1100	140	244	57.4
	3	78F	PD	3	1120	131	286	45.8
	4	80 M	PD	12	1140	259	459	56.4
	5	83F	PD	12	1320	117	261	44.8
	6	85F	PD	6	1240	114	177	65.0
	7	90F	PD	12	1140	143	229	62.4
Control	8	40 M	HCM	0.1 day	1320	69	910	7.6
	9	70 M	AMI	1 day	1140	63	1651	3.8
	10	76 M	Ear SCC	2	1240	85	766	11.1
	11	80 M	AMI	0.1 day	1210	38	1490	2.6

PD, Parkinson's disease; AMI, acute myocardial infarction; SCC, squamous cell carcinoma; HCM, hypertrophic cardiomyopathy.

by 24 h, PGE_2 had reached a maximal level that was about five-fold higher than the control value (Fig. 5A). On the other hand, 6-OHDA-induced PGE_2 production was completely absent in mesencephalic neurons derived from mPGES-1 KO mice, indicating that mPGES-1 is necessary for 6-OHDA-induced PGE_2 production. 6-OHDA also increased the levels of TXB_2, a stable metabolite of TXA_2, in WT neurons, while in mPGES-1 KO neurons, the basal levels of TXB_2 were higher than in WT neurons and were unchanged by 6-OHDA (Fig. 5B). The levels of 6-keto $PGF_{1\alpha}$, a stable metabolite of PGI_2, were not changed significantly by 6-OHDA in either WT or mPGES-1 KO neurons (Fig. 5C), suggesting that PGH_2, a substrate for mPGES-1, may be used to produce TXA_2 in mPGES-1 KO neurons. Neuronal death after 6-OHDA exposure in mPGES-1 KO neurons measured by MTT assay was less severe than that in WT neurons (Fig. 5D). Because only 6.42 ± 0.73% of total neurons were TH-positive dopaminergic neurons in our primary mesencephalic neuronal culture, the results from MTT assay could be attributed to the survival of other types of neurons and/or immature neurons than mature dopaminergic neurons. Therefore, survival of TH-positive dopaminergic neurons was also investigated by immunohistochemistry. TH-positive neurons were more vulnerable to 6-OHDA than other neurons (Fig. 5D and E). A decrease in the number of TH-positive cells after 6-OHDA exposure in mPGES-1 KO neurons was significantly less than that in WT neurons (Fig. 5E). As 6-OHDA is known to be oxidized as DA to generate free radicals and quinones in dopaminergic neurons (Mattammal et al., 1995; Asanuma and Miyazaki, 2006), we compared the amount of 8-isoprostane, a reliable indicator of oxidative stress, in WT and mPGES-1 KO neurons. 6-OHDA exposure resulted in an almost two-fold increase in 8-isoprostane production in WT neurons, while its production in mPGES-1 KO neurons was significantly lower than that in WT neurons and was not changed by 6-OHDA treatment (Fig. 5F). To investigate the effects of NS-398, a COX-2 specific inhibitor, and PGE_2 on 6-OHDA-induced neurotoxicity, we used lower concentration of 6-OHDA, because almost all TH-positive cells were disappeared regardless of genotypes by 72 h exposure of 30 μM 6-OHDA (Fig. 5E). Treatment with NS-398 prevented the neurotoxicity of 6-OHDA (5 μM) in WT neurons, while there was no effect on neuronal survival in mPGES-1 KO neurons that showed no 6-OHDA toxicity (Fig. 5G). Addition of PGE_2 significantly increased 6-OHDA-induced toxicity in mPGES-1 KO neurons, as well as in NS-398-treated WT neurons, to almost the same severity as that seen in 6-

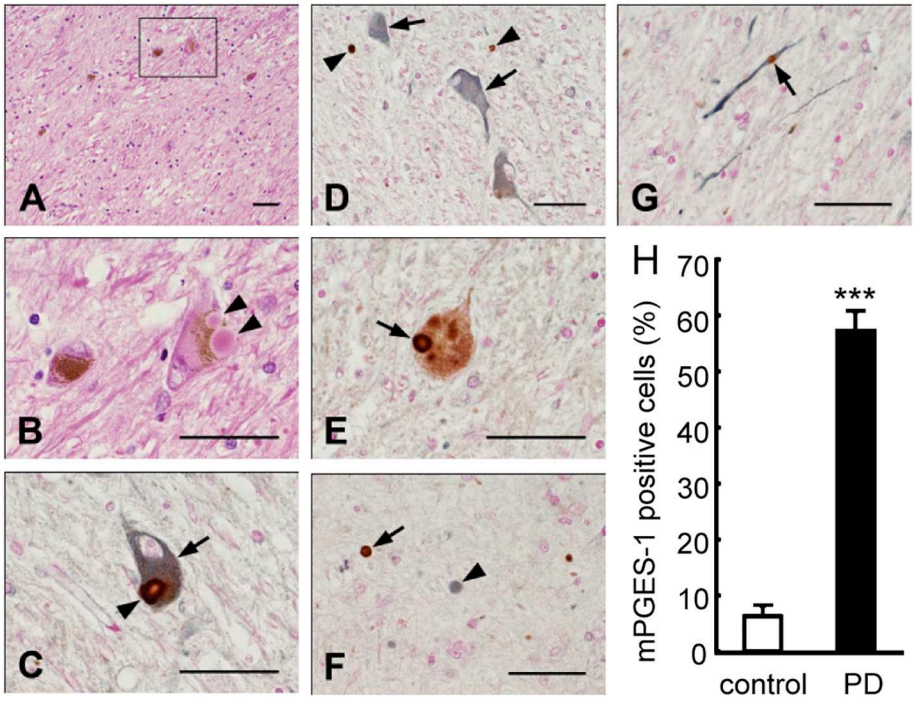

Fig. 3. mPGES-1 induction in dopaminergic neurons in the SNpc of postmortem brains from PD patients. A, Marked neuronal loss and fibrillary gliosis were evident in the SN stained by hematoxylin and eosin. B, A high-power view of the rectangular area in A showing a remaining neuron having characteristic Lewy bodies in the cytoplasm (arrowheads). C–G, Representative images of double-label immunohistochemistry using a labeled polymer method for α-synuclein with DAB (brown) and for mPGES-1 with SG (blue-gray) as chromogens, counterstained with Nuclear Fast Red. C, An mPGES-1-immunoreactive neuron (arrow: blue) with a cytoplasmic Lewy body that is strongly positive for α-synuclein (arrowhead: brown) but not for mPGES-1. D, mPGES-1-immunoreactive neurons (arrows) without Lewy bodies or α-synuclein-immunoreactivity. Note the cross-sections of putative α-synuclein-positive Lewy-related neurites (arrowheads) near these neurons. E, On rare occasions, there was a neuron that had multiple cytoplasmic Lewy bodies (arrow) without cytoplasmic mPGES-1 immunoreactivity. Note the weak but diffuse cytoplasmic immunoreactivity for α-synuclein. F, Cross-sections of an α-synuclein-immunoreactive neurite (arrow) and an mPGES-1-immunoreactive neurite (arrowhead). G, An α-synuclein-immunoreactive small Lewy body (arrow) within an mPGES-1-immunoreactive neurite. Bars in all panels indicate 50 μm. H, The ratio of mPGES-1-positive neurons was increased in PD. The positive ratio of mPGES-1 was defined as the percentage (%) of mPGES-1 immunoreactive neurons among the total number of neurons in the bilateral SN; n = 4 for control samples and n = 7 for PD samples, ***$p < .001$ vs. control (*t*-test). (For interpretation of the references to colour in this figure legend, the reader is referred to the web version of this article.)

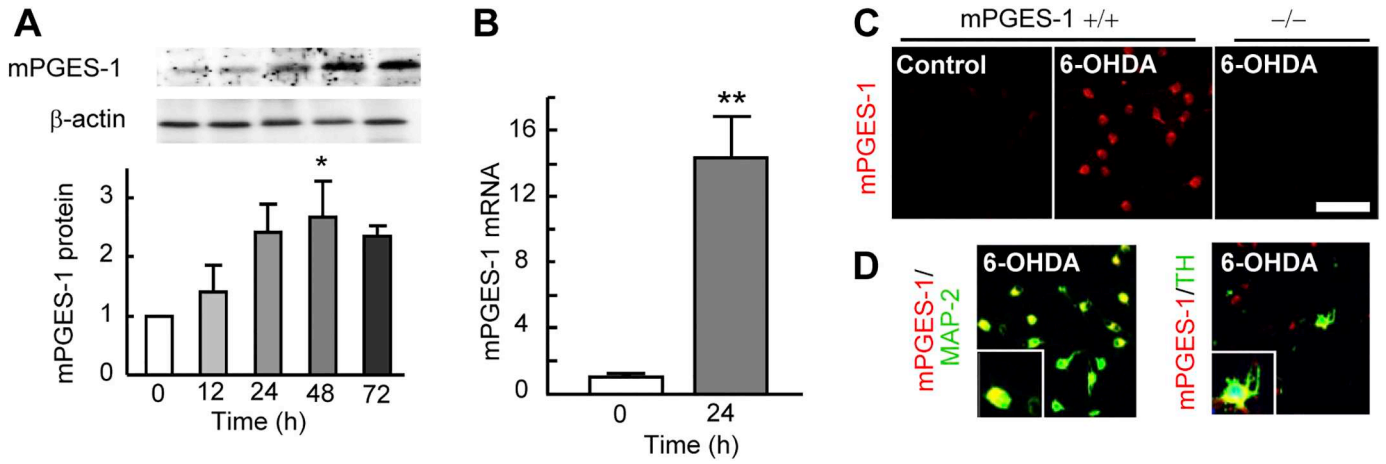

Fig. 4. mPGES-1 expression induced by 6-OHDA in mesencephalic neuronal cultures. A, Western blot analysis of the expression of mPGES-1 in cultured mesencephalic neurons exposed to 30 μM 6-OHDA for the indicated times. Bar graph: Quantitated data from immunoblotting with the mPGES-1 antibody were normalized to β-actin; n = 4. B, Real-time PCR analysis of the expression of mPGES-1 mRNA after exposure to 30 μM 6-OHDA for 24 h. Quantitated data for mPGES-1 mRNA levels were normalized to those for β-actin; n = 5, $^{**}p < .01$, $^{*}p < .05$ vs. 0 h. C, Expression of 30 μM 6-OHDA-induced mPGES-1 (red) is observed in WT (+/+) neurons, but not in mPGES-1 KO (−/−) neurons. Neurons were exposed to 6-OHDA for 72 h. D, Double-immunostaining of mPGES-1 (red) and MAP-2 and TH proteins (green) in the WT neurons exposed to 30 μM 6-OHDA for 72 h. Scale bar, 50 μm; insets, 12.5 μm. (For interpretation of the references to colour in this figure legend, the reader is referred to the web version of this article.)

OHDA-exposed WT neurons, while PGE_2 itself had no effect on the survival of neurons (data not shown). Taken together, these results suggest that induction of mPGES-1 enhances 6-OHDA-induced dopaminergic neuronal death by enhancing oxidative stress through excessive PGE_2 production.

3.4. mPGES-1 is necessary for PGE_2 production in the SN of 6-OHDA-lesioned mice

To evaluate the contribution of mPGES-1 to PGE_2 production in vivo, we used 6-OHDA-lesioned WT and mPGES-1 KO mice. In WT mice, significant PGE_2 production was observed in the SN at three days after 6-OHDA injection (Fig. 1C); thus, we compared levels of PGE_2 at three days after 6-OHDA injection between mPGES-1 KO and WT mice. The 6-OHDA-induced increase in PGE_2 levels observed in WT mice was completely absent in mPGES-1 KO mice (Fig. 6A), indicating that mPGES-1 plays a predominant role in 6-OHDA-induced PGE_2 production at the lesioned site. Basal PGE_2 content in mPGES-1 KO mice was lower than that in WT mice, but this was not significant. As the COX product PGH_2 serves as a common precursor to several prostanoids such as PGE_2, TXA_2, PGI_2, and PGD_2, deletion of mPGES-1 may cause shunting of surplus PGH_2 toward the remaining terminal PG synthases (Boulet et al., 2004; Leclerc et al., 2013). Thus, we measured TXB_2 and 6-keto $PGF_{1\alpha}$ as stable metabolites for TXA_2 and PGI_2, respectively, and PGD_2. TXB_2 was slightly increased by 6-OHDA injection in WT mice, but this was not significant (Fig. 6B). In mPGES-1 KO mice, basal TXB_2 levels were similar to those in WT mice, and were not changed by 6-OHDA injection. The levels of 6-keto $PGF_{1\alpha}$ were similar between WT and mPGES-1 KO mice with or without 6-OHDA injection (Fig. 6C). PGD_2 was slightly increased by 6-OHDA injection in both WT and mPGES-1 KO mice, but those were not significant (Fig. 6D). In mPGES-1 KO mice, PGD_2 levels were slightly less than those in WT mice, but those were also not significant. These results indicate that deletion of mPGES-1 causes no significant changes to prostanoids other than PGE_2. The induction of mPGES-1 in the SN after 6-OHDA injection in WT mice was absent in mPGES-1 KO mice; however, the expressions of mPGES-2, cPGES, COX-1, and COX-2 were similar in both WT and mPGES-1 KO mice (Fig. 6D), indicating that there was no compensatory up-regulation of other enzymes implicated in PGE_2 synthesis in mPGES-1 KO mice.

3.5. mPGES-1 contributes to dopaminergic neurodegeneration and neurological deficits in 6-OHDA-lesioned mice

To investigate the functional role of mPGES-1 in DA neurodegeneration in vivo, the effects of 6-OHDA in mPGES-1 KO mice were compared to those in WT mice. The number of TH-positive DA neurons did not differ between genotypes in the sham-operated SN; however, in mPGES-1 KO mice, significantly more TH-positive SNpc neurons survived after 6-OHDA injection compared to WT mice (Fig. 7A). We next assessed the integrity of the nigrostriatal pathway by retrograde Fluoro-Gold (FG) labeling in 6-OHDA-lesioned animals. FG labeling at 14 days after 6-OHDA injection showed profound loss of FG-labeled cells in the SNpc of WT mice, but not in mPGES-1 KO mice (Fig. 7B). In sham-operated animals, the number of FG-labeled neurons in the SNpc did not differ between genotypes. Similarly, striatal DA content at 14 days after 6-OHDA injection was significantly reduced in WT mice, but not in mPGES-1 KO mice (Fig. 7C). The decrease in DA content observed in lesioned WT mice lasted at least until 56 days after 6-OHDA injection. The DA content in the striatum of sham-operated animals did not differ between genotypes. As DA content was examined in the striatum where 6-OHDA was injected, a mechanical injury induced by the needle and vehicle injection could have occurred. Thus, we compared the DA content between a no-injection, no-surgery (NINS) group and a sham-operated group for both genotypes, and found no differences between those groups. The changes in DA content were reflected by an enhanced DA turnover observed only in the 6-OHDA-lesioned WT striatum as indicated by (HVA + DOPAC)/DA (data not shown). On the other hand, 5-HT and 5-HIAA content did not differ between genotypes or as a result of injection (data not shown). In both 6-OHDA-lesioned mice and PD patients, a decrease in striatal DA content caused by DA neurodegeneration in the SN is thought to underlie functional failure. To test the motor function of lesioned mice, the rotarod test was performed. In sham-operated mice, for both genotypes, almost all mice did not fall in the experimental period of 300 s; however, 6-OHDA lesioning induced a deficit in motor performance at 14 days after exposure in WT mice, but not in mPGES-1 KO mice (Fig. 7D). These results suggest that mPGES-1 contributes to motor deficits through enhancing DA neurodegeneration.

4. Discussion

Here, we have shown an up-regulation of mPGES-1 in nigrostriatal

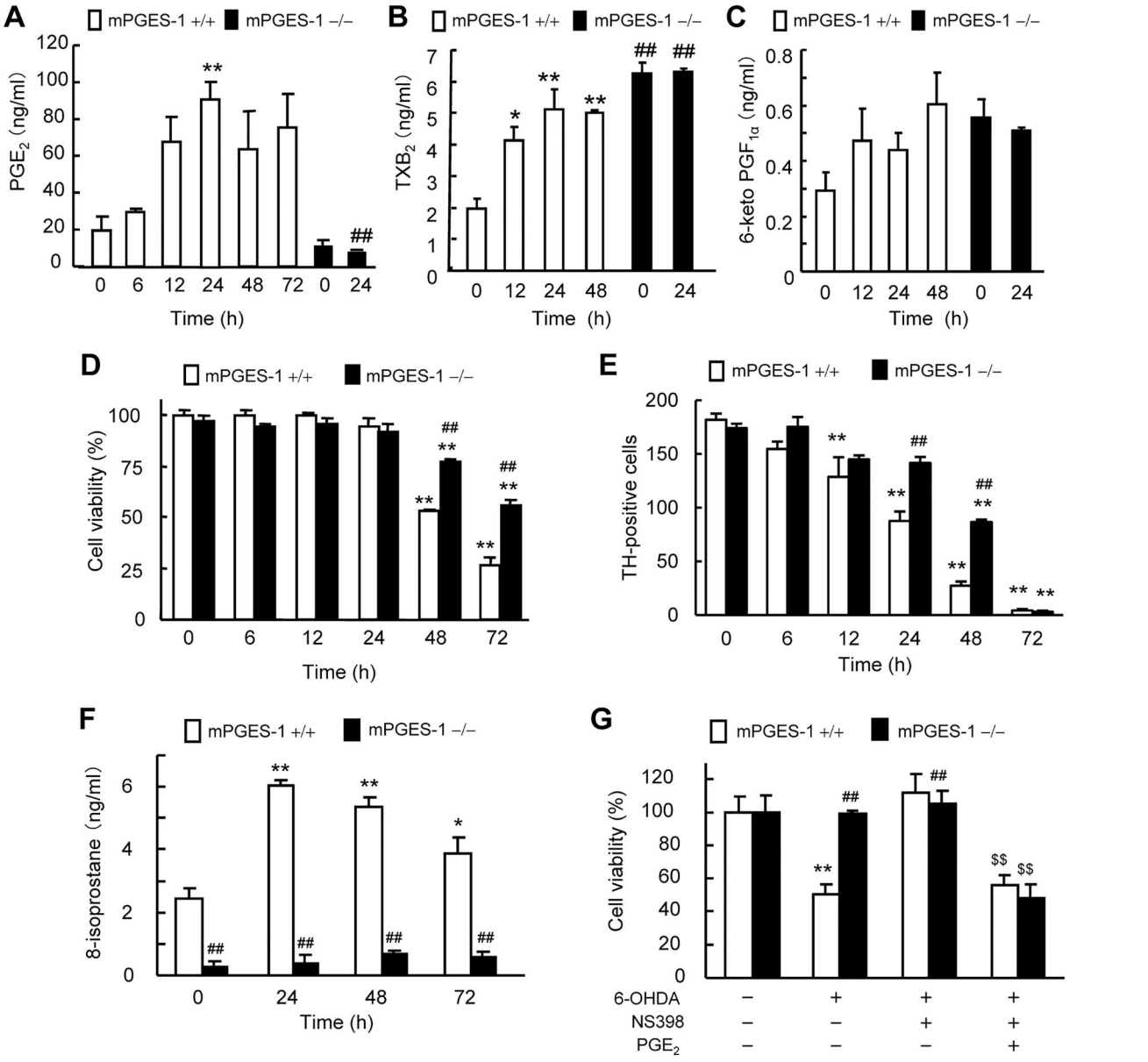

Fig. 5. mPGES-1 contributes to PGE_2 production and neuronal death induced by 6-OHDA in mesencephalic neuronal cultures. A-C, The production of PGE_2 (A), TXB_2 (B) and 6-keto $PGF_{1\alpha}$ (C) in the culture medium of mPGES-1 KO (−/−) and WT (+/+) neurons exposed to 30 μM 6-OHDA; n = 3, $^{*}p < .05$, $^{**}p < .01$ vs. 0 h, $^{\#\#}p < .01$ vs WT. D, The effects of 30 μM 6-OHDA exposure on cell viability in mPGES-1 KO (−/−) and WT (+/+) neurons; n = 5, $^{**}p < .01$ vs. 0 h, $^{\#\#}p < .01$ vs. WT. E, The effects of 30 μM 6-OHDA exposure on the number of TH-positive cells in the field (33 mm^2); n = 3, $^{**}p < .01$ vs. 0 h, $^{\#\#}p < .01$ vs. WT. F, The effects of 30 μM 6-OHDA exposure on oxidative stress in mPGES-1 KO (−/−) and WT (+/+) neurons; n = 5, $^{**}p < .01$ vs. 0 h, $^{\#\#}p < .01$ vs. WT. G, The effects of 5 μM NS-398 and 10 μM PGE_2 on 5 μM 6-OHDA-induced toxicity in mPGES-1 KO (−/−) and WT (+/+) neurons. 6-OHDA was exposed for 72 h; n = 3–5, $^{**}p < .01$ vs. control, $^{\#\#}p < .01$ vs. WT–6-OHDA, $^{\$\$}p < .01$ vs. 6-OHDA + NS-398.

dopaminergic neurons in both 6-OHDA-lesioned mice and human PD samples. Using mPGES-1 KO mice, we have also demonstrated that the production of PGE_2 through mPGES-1 induction plays a key role in the progression of dopaminergic neurodegeneration and neurological dysfunction in 6-OHDA-lesioned PD mice.

Although we could not detect any relationship between immunoreactivity for mPGES-1 and the presence of α-synuclein-positive Lewy bodies, significant mPGES-1 immunoreactivity was essentially found in SNpc dopaminergic neurons from PD mice and patients. This finding raises the possibility that mPGES-1 induction could amplify the neurodegenerative process specifically in SNpc dopaminergic neurons. Accumulated reports have been demonstrated the sex differences in PD patients and animal models of PD (Gillies et al., 2014). Because similar up-regulation of mPGES-1 mRNA were observed in both male and female substantia nigra of 6-OHDA-lesioned mice, and PGE_2 was up-regulated in both male and female mice, even that was not significant in female mice, it is suggested that mPGES-1 is involved in DA neurodegeneration regardless of sex both in PD patients and animal models of PD. We have previously demonstrated that intranigral injection of lipopolysaccharide (LPS) caused induction of mPGES-1 in activated (ameboid) microglia in the rat SN (Ikeda-Matsuo et al., 2005). Unlike the direct death of dopaminergic neurons caused by 6-OHDA, intranigral injection of LPS seems to cause indirect death due to an inflammatory reaction through microglial activation. Indeed, NF-κB, a transcription factor of mPGES-1 and COX-2, is activated in dopaminergic neurons and microglia in 6-OHDA-lesioned and LPS-lesioned animal models of PD, respectively (Liang et al., 2007; Zhang and Xu, 2018). In the brains of PD patients, COX-2 induction has been reported

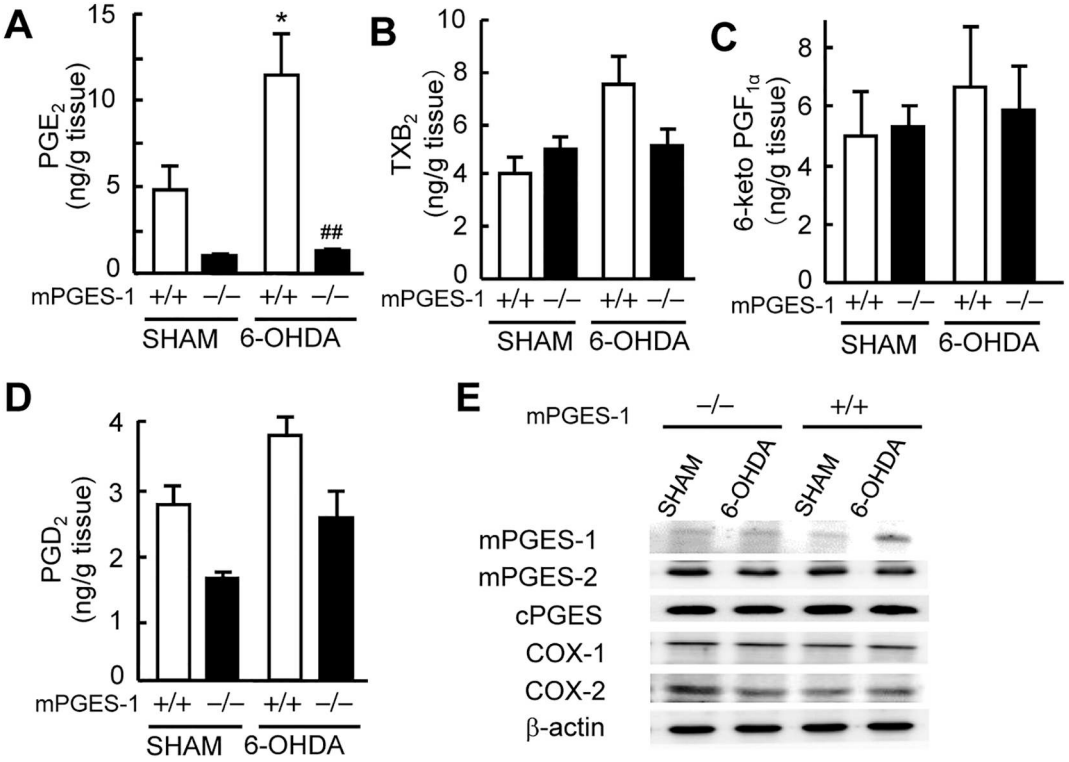

Fig. 6. mPGES-1 is essential for PGE_2 production in the SN in 6-OHDA-lesioned mice. A-D, The production of PGE_2 (A), TXB_2 (B), 6-keto $PGF_{1\alpha}$ (C) and PGD_2 (D) and in the SN of mPGES-1 KO (−/−) and WT (+/+) mice at 3 days after 6-OHDA injection and sham operation (SHAM); n = 3–5, $^{*}p < .05$ vs. SHAM, $^{\#\#}p < .01$ vs. WT. E, Western blot analyses for enzymes related to PGE_2 synthesis in the SN of mPGES-1 KO (−/−) and WT (+/+) mice at 14 days after 6-OHDA injection and sham operation (SHAM).

in either neurons or microglia, which seems to depend on the status of the neurodegeneration and whether neuroinflammation is predominant or not (Teismann et al., 2003; Knott et al., 2000). Therefore, in some PD patients, mPGES-1 may be up-regulated in microglia and contribute to dopaminergic neurodegeneration. However, as the data show here, mPGES-1 in dopaminergic neurons could be important for neurodegeneration in PD. Because mPGES-1-positive neurons were observed in the lesioned SN, the possibility that mPGES-1-positive dopaminergic neurons were survived after 6-OHDA injection because of protective role of mPGES-1 cannot be excluded. However, the fact that number of TH-positive neurons in mPEGS-1 KO mice was significantly higher than that in WT mice strongly suggests the neurodegenerative role of mPGES-1 in 6-OHDA-lesioned mice. Indeed, the induction of neuronal mPGES-1 contributes to 6-OHDA-induced neurotoxicity in cultured mesencephalic neurons, indicating that PGE_2 released by activated neurons through induction of mPGES-1 contributes to neurodegeneration in an autocrine manner. Increased mPGES-1 expression was associated with increased PGE_2 content in the SN of PD mice, indicating that mPGES-1 is catalytically active. As PGE_2 content in postmortem PD ventral midbrain samples is reported to be higher than in normal controls (Teismann et al., 2003), this suggests that the increased mPGES-1 expression observed here in the postmortem SNpc also results in increased catalytic activity. However, the time courses for mPGES-1 protein induction and PGE_2 production in PD mice were different. The transient increase in PGE_2 could be correlated with transient increases in the activities of mPGES-1 and the up-stream enzyme COX-2, which are known to be co-induced in the lesioned site of the brain and functionally coupled to produce high levels of PGE_2 (Murakami et al., 2002; Ikeda-Matsuo et al., 2010a). Nevertheless, 6-OHDA-induced PGE_2 production at 3 days after 6-OHDA injection was completely absent in mPGES-1 KO mice, indicating that small amount of mPGES-1 induction observed at 3 days is enough for local PGE_2 up-regulation and subsequent neurodegeneration. We have previously reported a similar difference between the time courses for mPGES-1 induction and PGE_2 production in an experimental model of brain ischemia (Ikeda-Matsuo et al., 2006). In the experiment using mesencephalic neuronal cultures, we show that induction of the mPGES-1 protein correlates with PGE_2 production. There may be posttranslational modulation of mPGES-1 activity and/or differences in the time courses of up-stream enzyme expressions involved in PGE_2 production, such as phospholipase A_2 and/or COX-2 in in vivo PD mice, as well as in vivo brain ischemia mice, and further studies are needed to clarify the mechanisms underlying the discordance between sustained mPGES-1 expression and transient PGE_2 production in vivo. mPGES-1 mRNA levels are also increased in the SN of PD mice, indicating that the induction of mPGES-1 is regulated at least in part at the transcription level. Indeed, two transcription factors, NF-κB and Egr-1, which have been demonstrated to be involved in transcriptional regulation of mPGES-1 (Barakat et al., 2009; Naraba et al., 2002), are known to be activated in the brain of 6-OHDA-lesioned rat model of PD (Martinez-Gonzalez et al., 2014; Liang et al., 2007). Importantly, increase in nuclear translocation of NF-κB in dopaminergic neurons of substantia nigra has been reported in the patients with PD (Hunot et al., 1997), suggesting that mPGES-1 is induced by transcriptional activation of NF-κB in dopaminergic neurons of PD patients. Although we found no apparent changes in the expression of cPGES or mPGES-2 in PD mice, the possibility that other types of PGES could contribute to PGE_2 production in the SN of 6-OHDA-lesioned mice cannot be excluded. However, the 6-OHDA-induced production of PGE_2 was completely absent in mPGES-1 KO mice, indicating that mPGES-1 plays a predominant role in PGE_2 production in the SN with dopaminergic neurodegeneration. The predominant role of mPGES-1 in PGE_2 production was also demonstrated in vitro using mesencephalic neurons, where increased production of PGE_2 by 6-OHDA stimulation was seen in WT neurons, but not in mPGES-1 KO neurons. No compensatory up-regulation of other enzymes implicated in PGE_2 synthesis was detected in mPGES-1 KO mice in vivo and in

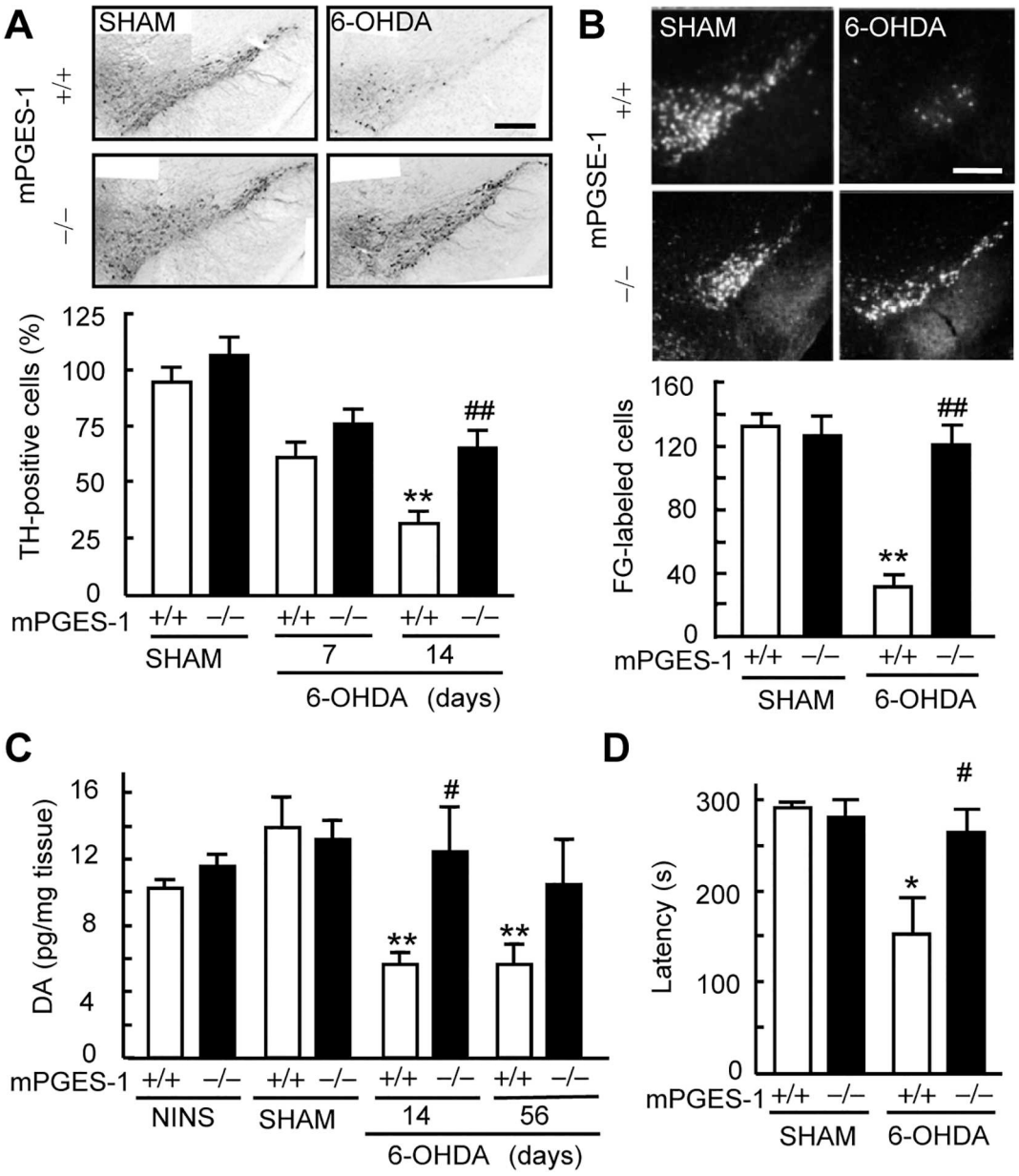

Fig. 7. Deletion of mPGES-1 resulted in marked amelioration of the dopaminergic neuronal loss, nigrostriatal projection impairment, DA deficiency, and motor dysfunction observed in 6-OHDA-lesioned mice. A, Representative TH-immunostained coronal sections of the SN of mPGES-1 KO (−/−) and WT (+/+) mice at 14 days after 6-OHDA injection and sham operation (SHAM). Scale bar, 250 μm. Bar graph: TH-positive neuronal counts were scaled to a percentage of the contralateral TH-positive cells; n = 5–8, $^{**}p < .01$ vs. SHAM, $^{\#\#}p < .01$ vs. WT. B, Representative FG-labeled coronal sections of the SN of mPGES-1 KO (−/−) and WT (+/+) mice at 14 days after 6-OHDA injection and sham operation (SHAM). Scale bar, 250 μm. Bar graph: The average number of FG-labeled cells; n = 5, $^{**}p < .01$ vs. SHAM, $^{\#\#}p < .01$ vs. WT. C, Striatal DA content in mPGES-1 KO (−/−) and WT (+/+) mice at 14 and 56 days after 6-OHDA injection, 14 days after a sham operation (SHAM) and in no-injection, no-surgery (NINS) controls. D, Effects of mPGES-1 deletion on the rotarod test in 6-OHDA-lesioned mice. Fourteen days after 6-OHDA injection, the latency (time) to falling off was recorded; n = 5–9, $^{*}p < .05$ vs. SHAM, $^{\#}p < .05$ vs. WT.

vitro. Although PGI_2, TXA_2 and PGD_2 are produced from the same precursor as PGE_2, and deletion of mPGES-1 caused up-regulation of basal level of TXA_2 in vitro, no shunting of surplus PGH_2 toward the production of PGI_2, TXA_2 and PGD_2 were observed in vivo PD mice brain. The genetic deletion of mPGES-1 ameliorated dopaminergic neuronal loss, the decrease in DA content and disruption of the nigrostriatal pathway, along with motor dysfunction in lesioned mice, suggesting that mPGES-1 is a critical factor in the progression of dopaminergic neurodegeneration and related neurological dysfunction.

In recent studies, COX-2-deficient mice showed attenuated dopaminergic neurodegeneration with decreased production of not only PGE_2 but also 5-cysteinyl-dopamine, a stable metabolite engendered by the COX-related oxidation of DA (Teismann et al., 2003). As both PGE_2 and oxidized DA are thought to be neurotoxic (Asanuma and Miyazaki, 2006), it was unclear which of these was important for COX-2-associated neurotoxicity in PD mice. The phenotype of the toxin-induced PD model in mPGES-1 KO mice resembles that of COX-2 KO mice, both showing reduction in PGE_2 production, protection of dopaminergic neurons in SN and amelioration of behavioral neurological deficits, suggesting that coordinated induction of mPGES-1 and COX-2 is required for excessive PGE_2 production in the SN, which causes dopaminergic neurodegeneration. In fact, we observed here the co-localization of mPGES-1 and COX-2 in the SNpc dopaminergic neurons of lesioned mice. In vitro analysis using a COX-2 inhibitor and exogenous

PGE_2 in WT and mPGES-1 KO mesencephalic neurons clearly shows that both neuronal mPGES-1 and COX-2 are required for neurotoxic PGE_2 production. As mPGES-1 KO neurons showed less oxidative stress than WT neurons as indicated by the levels of 8-isoprostane, PGE_2 produced by up-regulation of mPGES-1 in the SN of PD patients may enhance oxidative stress that has occurred in dopaminergic neurons, thereby resulting in a deterioration of neurodegeneration.

PGE_2 can efflux by simple diffusion or by a PGE_2 efflux transporter after synthesis and can activate four G protein-coupled receptors (EP1–4) with quite different signaling cascades. EP1 and EP3 receptors appear to be essential for the neurotoxicity mediated by PGE_2, while the EP2 receptor appears to be protective, determining the scope of acute neuronal injury in stroke (Kawano et al., 2006; Ikeda-Matsuo et al., 2010b, 2011; McCullough et al., 2004). In the rat SN, immunostaining for EP receptors revealed that EP1 and EP2 receptors are expressed in DA neurons, while EP3 receptors, as well as a part of the EP2 receptors, are expressed in non-DA neurons (Carrasco et al., 2007). It was recently demonstrated using EP1-deficient mice that the EP1 receptor is essential for dopaminergic neurodegeneration and behavioral dysfunction in the 6-OHDA-induced PD model (Ahmad et al., 2013). Conversely, activation of EP2 by a specific agonist was shown to protect dopaminergic neurons against 6-OHDA-induced toxicity through protein kinase A (Carrasco et al., 2008). Recently, anti-inflammatory and neuroprotective effect of EP4 signaling in a MPTP-induced PD has been also reported (Pradhan et al., 2017). Thus, timing, localization and/or amount of PGE_2 could be important to determine whether PGE_2 causes neuroprotective or neurotoxic effect in PD brain. Although further study will be needed to identify the mechanisms by which mPGES-1 affects neurotoxicity, the present study provides new insight that endogenous PGE_2 produced in the SN accelerates dopaminergic neurodegeneration.

5. Conclusions

We have shown that mPGES-1 is induced in DA neurons in the SNpc of both the 6-OHDA-induced PD mouse model and PD postmortem specimens, and that mPGES-1 plays a critical role not only in PGE_2 production but also in the dopaminergic neurodegeneration and behavioral dysfunction seen in PD mice. Considering that COX inhibitors can non-selectively suppress the production of many types of prostanoids that are essential for normal physiological functions within the brain (Kaufmann et al., 1997) and other tissues (Poorani et al., 2016), thereby inducing gastrointestinal, renal, and cardiovascular complications, mPGES-1 inhibitors are expected to be injury-selective with fewer side-effects (Korotkova and Jakobsson, 2014). Thus, mPGES-1 may be a valuable target for the development of new therapies for PD aimed at slowing progression of the neurodegenerative process.

Acknowledgements

This work was partially supported by KAKENHI (24590121, Y·I-M), the Uehara Memorial Foundation (2009-166, Y·I-M), and Hokuriku University Special Research Grant (Y·I-M).

References

Ahmad, A.S., Maruyama, T., Narumiya, S., Doré, S., 2013. PGE(2) EP1 Receptor Deletion Attenuates 6-OHDA-Induced Parkinsonism in mice: Old Switch, New Target. Neurotox. Res. 23, 260–266. https://doi.org/10.1007/s12640-013-9381-8.

Asanuma, M., Miyazaki, I., 2006. Nonsteroidal anti-inflammatory drugs in Parkinson's disease: possible involvement of quinone formation. Expert. Rev. Neurother. 6, 1313–1325. https://doi.org/10.1586/14737175.6.9.1313.

Baba, M., Nakajo, S., Tu, P.H., Tomita, T., Nakaya, K., Lee, V.M., Trojanowski, J.Q., Iwatsubo, T., 1998. Aggregation of α-synuclein in Lewy bodies of sporadic Parkinson's disease and dementia with Lewy bodies. Am. J. Pathol. 152, 879–884.

Barakat, W., Herrmann, O., Baumann, B., Schwaninger, M., 2009. NF-kappaB induces PGE_2-synthesizing enzymes in neurons. Naunyn Schmiedeberg's Arch. Pharmacol. 380, 153–160. https://doi.org/10.1007/s00210-009-0421-0.

Boulet, L., Ouellet, M., Bateman, K.P., Ethier, D., Percival, M.D., Riendeau, D., Mancini, J.A., Méthot, N., 2004. Deletion of microsomal prostaglandin E2 (PGE2) synthase-1 reduces inducible and basal PGE2 production and alters the gastric prostanoid profile. J. Biol. Chem. 279, 23229–23237. https://doi.org/10.1074/jbc.M400443200.

Carrasco, E., Casper, D., Werner, P., 2007. PGE2 receptor EP1 renders dopaminergic neurons selectively vulnerable to low-level oxidative stress and direct PGE2 neurotoxicity. J. Neurosci. Res. 85, 3109–3117. https://doi.org/10.1002/jnr.21425.

Carrasco, E., Werner, P., Casper, D., 2008. Prostaglandin receptor EP2 protects dopaminergic neurons against 6-OHDA-mediated low oxidative stress. Neurosci. Lett. 441, 44–49. https://doi.org/10.1016/j.neulet.2008.05.111.

Deleidi, M., Gasser, T., 2013. The role of inflammation in sporadic and familial Parkinson's disease. Cell. Mol. Life Sci. 70, 4259–4273. https://doi.org/10.1007/s00018-013-1352-y.

Engblom, D., Saha, S., Engström, L., Westman, M., Audoly, L.P., Jakobsson, P.J., Blomqvist, A., 2003. Microsomal prostaglandin E synthase-1 is the central switch during immune-induced pyresis. Nat. Neurosci. 6, 1137–1138. https://doi.org/10.1038/nn1137.

Gillies, G.E., Pienaar, I.S., Vohra, S., Qamhawi, Z., 2014. Sex differences in Parkinson's disease. Front. Neuroendocrinol. 35, 370–384. https://doi.org/10.1016/j.yfrne.2014.02.002.

Hunot, S., Brugg, B., Ricard, D., Michel, P.P., Muriel, M.P., Ruberg, M., Faucheux, B.A., Agid, Y., Hirsch, E.C., 1997. Nuclear translocation of NF-kappaB is increased in dopaminergic neurons of patients with parkinson disease. Proc. Natl. Acad. Sci. U. S. A. 94, 7531–7536.

Ikeda, Y., Nishiyama, N., Saito, H., Katsuk, I.H., 1997. GABAA receptor stimulation promotes survival of embryonic rat striatal neurons in culture. Brain Res. Dev. Brain Res. 98, 253–258.

Ikeda, Y., Ueno, A., Naraba, H., Matsuki, N., Oh-Ishi, S., 2000. Intracellular Ca^{2+} increase in neuro-2A cells and rat astrocytes following stimulation of bradykinin B2 receptor. Jpn. J. Pharmacol. 84, 140–145.

Ikeda-Matsuo, Y., Ikegaya, Y., Matsuki, N., Uematsu, S., Akira, S., Sasaki, Y., 2005. Microglia-specific expression of microsomal prostaglandin E2 synthase-1 contributes to lipopolysaccharide-induced prostaglandin E2 production. J. Neurochem. 94, 1546–1558. https://doi.org/10.1111/j.1471-4159.2005.03302.x.

Ikeda-Matsuo, Y., Ota, A., Fukada, T., Uematsu, S., Akira, S., Sasaki, Y., 2006. Microsomal prostaglandin E synthase-1 is a critical factor of stroke-reperfusion injury. Proc. Natl. Acad. Sci. U. S. A. 103, 11790–11795. https://doi.org/10.1073/pnas.0604400103.

Ikeda-Matsuo, Y., Hirayama, Y., Ota, A., Uematsu, S., Akira, S., Sasaki, Y., 2010a. Microsomal prostaglandin E synthase-1 and cyclooxygenase-2 are both required for ischaemic excitotoxicity. Br. J. Pharmacol. 159, 1174–1186. https://doi.org/10.1111/j.1476-5381.2009.00595.x.

Ikeda-Matsuo, Y., Tanji, H., Ota, A., Hirayama, Y., Uematsu, S., Akira, S., Sasaki, Y., 2010b. Microsomal prostaglandin E synthase-1 contributes to ischaemic excitotoxicity through prostaglandin E2 EP3 receptors. Br. J. Pharmacol. 160, 847–859. https://doi.org/10.1111/j.1476-5381.2010.00711.x.

Ikeda-Matsuo, Y., Tanji, H., Narumiya, S., Sasaki, Y., 2011. Inhibition of prostaglandin E2 EP3 receptors improves stroke injury via anti-inflammatory and anti-apoptotic mechanisms. J. Neuroimmunol. 238, 34–43. https://doi.org/10.1016/j.jneuroim.2011.06.014.

Jakobsson, P.J., Thoren, S., Morgenstern, R., Samuelsson, B., 1999. Identification of human prostaglandin E synthase: a microsomal, glutathione-dependent, inducible enzyme, constituting a potential novel drug target. Proc. Natl. Acad. Sci. U. S. A. 96, 7220–7225.

Kamei, D., Yamakawa, K., Takegoshi, Y., Mikami-Nakanishi, M., Nakatani, Y., Oh-Ishi, S., Yasui, H., Azuma, Y., Hirasawa, N., Ohuchi, K., Kawaguchi, H., Ishikawa, Y., Ishii, T., Uematsu, S., Akira, S., Murakami, M., Kudo, I., 2004. Reduced pain hypersensitivity and inflammation in mice lacking microsomal prostaglandin e synthase-1. J. Biol. Chem. 279, 33684–33695. https://doi.org/10.1074/jbc.M400199200.

Kaufmann, W.E., Andreasson, K.I., Isakson, P.C., Worley, P.F., 1997. Cyclooxygenases and the central nervous system. Prostaglandins 54, 601–624.

Kawano, T., Anrather, J., Zhou, P., Park, L., Wang, G., Frys, K.A., Kunz, A., Cho, S., Orio, M., Iadecola, C., 2006. Prostaglandin E2 EP1 receptors: downstream effectors of COX-2 neurotoxicity. Nat. Med. 12, 225–229. https://doi.org/10.1038/nm1362.

Knott, C., Stern, G., Wilkin, G.P., 2000. Inflammatory regulators in Parkinson's disease: iNOS, lipocortin-1, and cyclooxygenases-1 and -2. Mol. Cell. Neurosci. 16, 724–739. https://doi.org/10.1006/mcne.2000.0914.

Korotkova, M., Jakobsson, P.J., 2014. Characterization of microsomal prostaglandin E synthase 1 inhibitors. Basic Clin. Pharmacol. Toxicol. 114, 64–69. https://doi.org/10.1111/bcpt.12162.

Leclerc, P., Idborg, H., Spahiu, L., Larsson, C., Nekhotiaeva, N., Wannberg, J., Stenberg, P., Korotkova, M., Jakobsson, P.J., 2013. Characterization of a human and murine mPGES-1 inhibitor and comparison to mPGES-1 genetic deletion in mouse models of inflammation. Prostaglandins Other Lipid Mediat. 107, 26–34. https://doi.org/10.1016/j.prostaglandins.2013.09.001.

Liang, Z.Q., Li, Y.L., Zhao, X.L., Han, R., Wang, X.X., Wang, Y., Chase, T.N., Bennett, M.C., Qin, Z.H., 2007. NF-kappaB contributes to 6-hydroxydopamine-induced apoptosis of nigral dopaminergic neurons through p53. Brain Res. 1145, 190–203. https://doi.org/10.1016/j.brainres.2007.01.130.

Lima, M.M., Reksidler, A.B., Zanata, S.M., Machado, H.B., Tufik, S., Vital, M.A., 2006. Different parkinsonism models produce a time-dependent induction of COX-2 in the substantia nigra of rats. Brain Res. 1101, 117–125. https://doi.org/10.1016/j.brainres.2006.05.016.

Magrinelli, F., Picelli, A., Tocco, P., Federico, A., Roncari, L., Smania, N., Zanette, G., Tamburin, S., 2016. Pathophysiology of motor dysfunction in Parkinson's disease as the rationale for drug treatment and rehabilitation. Parkinsons Dis. 2016, 9832839. https://doi.org/10.1155/2016/9832839.

Martinez-Gonzalez, C., Vvan Andel, J., Bolam, J.P., Mena-Segovia, J., 2014. Divergent motor projections from the pedunculopontine nucleus are differentially regulated in

Parkinsonism. Brain Struct. Funct. 219, 1451–1462. https://doi.org/10.1007/s00429-013-0579-6.

Mattammal, M.B., Strong, R., Lakshmi, V.M., Chung, H.D., Stephenson, A.H., 1995. Prostaglandin H synthetase-mediated metabolism of dopamine: implication for Parkinson's disease. J. Neurochem. 64, 1645–1654.

McCullough, L., Wu, L., Haughey, N., Liang, X., Hand, T., Wang, Q., Breyer, R.M., Andreasson, K., 2004. Neuroprotective function of the PGE2 EP2 receptor in cerebral ischemia. J. Neurosci. 24, 257–268. https://doi.org/10.1523/JNEUROSCI.4485-03.2004.

Murakami, M., Naraba, H., Tanioka, T., Semmyo, N., Nakatani, Y., Kojima, F., Ikeda, T., Fueki, M., Ueno, A., Oh-Ishi, S., Kudo, I., 2000. Regulation of prostaglandin E2 biosynthesis by inducible membrane-associated prostaglandin E2 synthase that acts in concert with cyclooxygenase-2. J. Biol. Chem. 275, 32783–32792. https://doi.org/10.1074/jbc.M003505200.

Murakami, M., Nakatani, Y., Tanioka, T., Kudo, I., 2002. Prostaglandin E synthase. Prostaglandins Other Lipid Mediat. 68-69, 383–399.

Naraba, H., Yokoyama, C., Tago, N., Murakami, M., Kudo, I., Fueki, M., Oh-Ishi, S., Tanabe, T., 2002. Transcriptional regulation of the membrane-associated prostaglandin E_2 synthase gene. Essential role of the transcription factor Egr-1. J. Biol. Chem. 277, 28601–28608. https://doi.org/10.1074/jbc.M203618200.

Poorani, R., Bhatt, A.N., Dwarakanath, B.S., Das, U.N., 2016. COX-2, aspirin and metabolism of arachidonic, eicosapentaenoic and docosahexaenoic acids and their physiological and clinical significance. Eur. J. Pharmacol. 785, 116–132. https://doi.org/10.1016/j.ejphar.2015.08.049.

Pradhan, S.S., Salinas, K., Garduno, A.C., Johansson, J.U., Wang, Q., Manning-Bog, A., Andreasson, K.I., 2017. Anti-inflammatory and neuroprotective effects of PGE_2 EP4 signaling in models of Parkinson's disease. J. NeuroImmune Pharmacol. 12, 292–304. https://doi.org/10.1007/s11481-016-9713-6.

Reksidler, A.B., Lima, M.M., Zanata, S.M., Machado, H.B., da Cunha, C., Andreatini, R., Tufik, S., Vital, M.A., 2007. The COX-2 inhibitor parecoxib produces neuroprotective effects in MPTP-lesioned rats. Eur. J. Pharmacol. 560, 163–175. https://doi.org/10.1016/j.ejphar.2006.12.032.

Sánchez-Pernaute, R., Ferree, A., Cooper, O., Yu, M., Brownell, A.L., Isacson, O., 2004. Selective COX-2 inhibition prevents progressive dopamine neuron degeneration in a rat model of Parkinson's disease. J. Neuroinflammation 1, 6. https://doi.org/10.1186/1742-2094-1-6.

Teismann, P., Tieu, K., Choi, D.K., Wu, D.C., Naini, A., Hunot, S., Vila, M., Jackson-Lewis, V., Przedborski, S., 2003. Cyclooxygenase-2 is instrumental in Parkinson's disease neurodegeneration. Proc. Natl. Acad. Sci. U. S. A. 100, 5473–5478. https://doi.org/10.1073/pnas.0837397100.

Tufekci, K.U., Meuwissen, R., Genc, S., Genc, K., 2012. Inflammation in Parkinson's disease. Adv. Protein Chem. Struct. Biol. 88, 69–132. https://doi.org/10.1016/B978-0-12-398314-5.00004-0.

Uematsu, S., Matsumoto, M., Takeda, K., Akira, S., 2002. Lipopolysaccharide-dependent prostaglandin E(2) production is regulated by the glutathione-dependent prostaglandin E(2) synthase gene induced by the Toll-like receptor 4/MyD88/NF-IL6 pathway. J. Immunol. 168, 5811–5816.

Yildirim, F.B., Ozsoy, O., Tanriover, G., Kaya, Y., Ogut, E., Gemici, B., Dilmac, S., Ozkan, A., Agar, A., Aslan, M., 2014. Mechanism of the beneficial effect of melatonin in experimental Parkinson's disease. Neurochem. Int. 79, 1–11. https://doi.org/10.1016/j.neuint.2014.09.005.

Zhang, F.X., Xu, R.S., 2018. Juglanin ameliorates LPS-induced neuroinflammation in animal models of Parkinson's disease and cell culture via inactivating TLR4/NF-κB pathway. Biomed. Pharmacother. 97, 1011–1019. https://doi.org/10.1016/j.biopha.2017.08.132.